

ON OPERATION CAPABILITIES ANALYSIS OF A 100000 TDW TANKER BY SEAKEEPING CRITERIA

Leonard Domnișorù

“Dunarea de Jos” University of Galati,
Faculty of Naval Architecture,
Galati, Domneasca Street, No. 47, 800008, Romania,
E-mail: leonard.domnisoru@ugal.ro

ABSTRACT

The operation capabilities of a maritime ship have to be assessed during the design, including the seakeeping criteria. In this study a 100000 tdw tanker is considered, with two loading conditions, cargo and ballast. The numerical analyses are developed with our own software DYN, module OSC, based on a linear hydrodynamic strip theory. The main oscillation components, heave, pitch and roll, are considered. The analysis includes an extended parametric study for the tanker speed up to 15 knots, different vertical positions of the gravity centre, a heading angle full range and irregular waves significant height up to 12m. Also the seakeeping limits have two sets of criteria. The results are pointing out the operation limits of the tanker on combined navigation parameters in irregular waves, by motions and acceleration short term seakeeping criteria.

Keywords: ship oscillations, tanker ship, irregular waves, seakeeping criteria, parametric study.

1. INTRODUCTION

The development of the design concept for a maritime ship involves many criteria to be assessed, according to the design rules of the ship's classification societies [4],[5],[13].

In this study the seakeeping analysis [1], [2],[10],[11],[14] is selected, for an extended parametric study of the operation capabilities evaluation of a 100000 tdw tanker [8].

The following main parameters are considered: loading case Δ , x_G , cargo (TK1) and ballast (TK2); speed v , 0, 5, 10, 12.5, and 15 kn; the theoretical vertical position of the gravity centre z_G , 8, 9, 10, 11, 12, 13 and 14 m; tanker-wave heading angle μ , 0-360 deg, step 5 deg; irregular waves significant height H_s , 0-12 m, step 0.05 m. In addition, two sets of limit values for the seakeeping criteria are considered.

The study ship, a 100000 tdw tanker [8], has the transversal offset-lines illustrated in Fig.1 and the main characteristics shown in Table 1.

Figs.2.a,b and Tables 2.b present the transversal stability data and the natural periods for roll oscillations, for the z_G theoretical range.

The seakeeping simulations are done by our own program DYN [6], module OSC, for ship's oscillations in regular and irregular waves, statistical short-term results, based on a linear strip theory hydrodynamic model, presented in brief in section 2. The program DYN-OSC has been previously validated by several experimental tests on scaled models, at towing tank, in regular head, follow and beam wave conditions, with the results presented in references [3],[7],[19],[12]. The parametric study aims to test the sensitivity of the operation limits of the 100000 tdw tank, due to the changes of several navigation data.

The dynamic response in regular waves of the 100000 tdw tankers, in terms of the response amplitude operators [1],[14], is presented in section 3. The dynamic response in irregular waves and seakeeping criteria assessment [6],[11] are presented in section 4.

The conclusions of this study (section 5) synthesize the 100000 tdw tanker operation limits parametric study by seakeeping criteria.

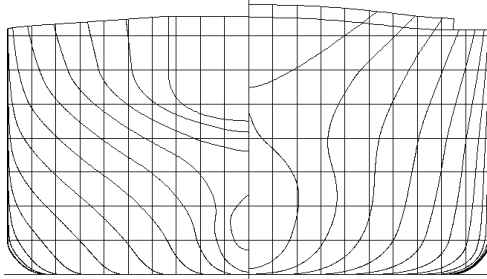


Fig.1. The 100000 tdw tank offset-lines [8]

Table 1. The 100000 tdw tank main data [8]

$L_{OA}[\text{m}]$	246	Case:	TK1cargo	TK2ballast
$B[\text{m}]$	42	$\Delta[\text{t}]$	126457	81763
$H[\text{m}]$	21.3	$x_G[\text{m}]$	126.4	128.3
$\rho[\text{t/m}^3]$	1.025	$L_{WL}[\text{m}]$	240	232
$g[\text{m/s}^2]$	9.81	$d_m[\text{m}]$	15	10
$H_{max}[\text{m}]$	12	$T_3[\text{s}]$	10.333	9.336
stations	41	$T_5[\text{s}]$	10.517	9.796
points	1230	$z_G[\text{m}]$	8 – 14 (step 1)	
$v_{max}[\text{kn}]$	15	$\mu [\text{deg}]$	0 – 360 (step 5)	

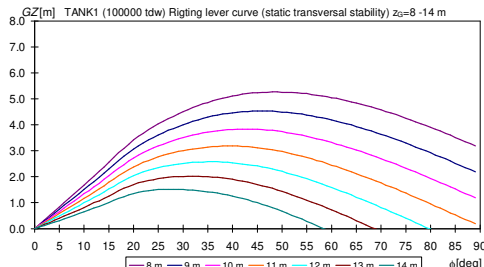


Fig.2.a. $GZ[\text{m}]$, TK1, $d_m=15\text{m}$, $z_G=8-14 \text{ m}$

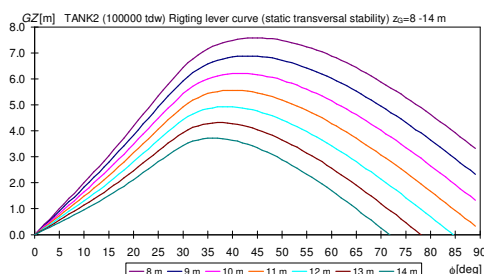


Fig.2.b. $GZ[\text{m}]$, TK2, $d_m=10\text{m}$, $z_G=8-14 \text{ m}$

Table 2.a TK1, stability data and roll periods

$z_G[\text{m}]$	$GM_{T0}[\text{m}]$	$J_x[\text{tm}^2]$	$T_4[\text{s}]$	$\phi_{maxGZ}[\text{deg}]$
8	9.562	21286956	9.631	49
9	8.562	22003546	10.334	46
10	7.562	22804441	11.181	43
11	6.562	23689642	12.233	39
12	5.562	24659147	13.547	36
13	4.562	25712956	15.255	32
14	3.562	26851071	17.564	28

Table 2.b TK2, stability data and roll periods

$z_G[\text{m}]$	$GM_{T0}[\text{m}]$	$J_x[\text{tm}^2]$	$T_4[\text{s}]$	$\phi_{maxGZ}[\text{deg}]$
8	11.303	13763496	10.468	45
9	10.303	14226821	11.223	43
10	9.303	14744656	12.074	41
11	8.303	15316999	13.005	40
12	7.303	15943851	14.018	39
13	6.303	16625213	15.265	37
14	5.303	17361083	16.846	36

2. THEORETICAL FUNDAMENTS

The seakeeping analysis with our own program DYN [6], module OSC, based on a linear strip theory 2D hydrodynamic model [2],[6],[14], has three main steps.

- Dynamic response in regular waves, when the response amplitude operators RAO are obtained by a direct solution in the frequency domain of the motions equations system:

$$[A]\{\ddot{p}(t)\} + [B]\{\dot{p}(t)\} + [C]\{p(t)\} = \{E_w(t)\} \quad (1)$$

$$\{E_w(t)\} = \{E_w^c\} \cos \omega_e t + \{E_w^s\} \sin \omega_e t \rightarrow$$

$$p_j(t) = p_j^c \cos \omega_e t + p_j^s \sin \omega_e t \quad j = 3,4,5 \quad (2)$$

$$p_j^a = \sqrt{(p_j^c)^2 + (p_j^s)^2}; \quad \omega_e = \omega - \frac{\omega^2}{g} v \cos \mu \quad (3)$$

$$RAO_j(\omega_e) = p_j^a(\omega_e) \Big|_{aw=1} \quad j = 3,4,5$$

where: $[A], [B], [C]$ are the radiation matrix; $\{E_w(t)\}$ is the regular wave diffraction vector; $\{p(t)\}$ is the dynamic response; ω_e is the wave encountering frequency; ω, μ are the regular wave frequency and heading angle; v is the ship speed; $RAO_j(\omega_e) \quad j = 3,4,5$ are the heave, roll and pitch RAO functions.

- Dynamic response in irregular waves, when the most probable short-term statistical motions RMS_j (5) and acceleration RMS_{acj} (6) amplitudes are obtained:

$$S_j(\omega_e) = RAO_j^2(\omega_e) S_w(\omega_e) \quad j = 3,4,5 \quad (4)$$

$$RMS_j = \left(\int_{(\omega_e)} S_j(\omega_e) d\omega_e \right)^{0.5} \quad j = 3,4,5 \quad (5)$$

$$RMS_{acj} = \left(\int_{(\omega_e)} \omega_e^4 S_j(\omega_e) d\omega_e \right)^{0.5} \quad j = 3,4,5 \quad (6)$$

where: S_w is the wave power density spectrum, ITTC [10] (Fig.9); S_j is the response spectrum.

- The polar diagrams of wave height significant and Beaufort level limits (7) by seakeeping criteria (8) – (11) are obtained, with two sets of admissible values from Table 3:

$$H_{s\lim}(\Delta, v, \mu); B_{\lim}(\Delta, v, \mu) \quad (7)$$

$$RMS_Z = RMS_3 + \xi_{amf} RMS_5 + \frac{B}{2} RMS_4 + \frac{H_s}{4}$$

$$\xi_{aft} = x_F; \xi_{mid} = 0; \xi_{fore} = L - x_F \quad (8)$$

$$RMS_{zadm} = H - f_s - d \Big|_{aft, mid, fore} f_s = 0.3m$$

$$RMS_Z \leq RMS_{zadm} \Big|_{aft, mid, fore} \quad (9)$$

$$RMS_{ac3} \leq RMS_{ac3adm} = 0.1g$$

$$RMS_4 \leq RMS_{4adm} = 6 - 8 \text{ deg}$$

$$RMS_{ac4} \leq RMS_{ac4adm} = 0.15g/(B/2) \quad (10)$$

$$RMS_5 \leq RMS_{5adm} = 3 - 4 \text{ deg}$$

$$RMS_{ac5} \leq RMS_{ac5adm} = 0.15g/\min\{\xi_{aft}, \xi_{fore}\} \quad (11)$$

where: x_F is the reference still water plane centre longitudinal position ($x=0, L$).

Table 3 Seakeeping criteria admissible values

Limits version	Criteria A	Criteria B
$RMS_{Zaft\ adm}$ [m]	7.3	7.8
$RMS_{Zmid\ adm}$ [m]	6.0	6.5
$RMS_{Zfore\ adm}$ [m]	7.7	8.2
$RMS_{5\ adm}$ [rad]	0.05236	0.06981
$RMS_{4\ adm}$ [rad]	0.10472	0.13963
$RMS_{ac3\ adm}$ [m/s ²]	0.981	0.981
$RMS_{ac5\ adm}$ [rad/s ²]	0.01224	0.01224
$RMS_{ac4\ adm}$ [rad/s ²]	0.07007	0.07007

3. DYNAMIC RESPONSE IN REGULAR WAVES

The dynamic response in regular waves is computed for a wave frequency range of $\omega=0-3$ rad/s, step 0.001 rad/s and wave amplitude $a_w=1$ m, covering the whole oscillations range frequencies of heave, pitch and roll motions. Using equations (1)-(3), the RAO response amplitude operators are obtained by DYN [6], module OSC, for the parametric study defined in section 1.

3.1 Loading case TK1

Figs.3.a-d present a selection of heave RAO_3 for the loading case TK1. The maximum heave results are at at head-quarter wave, $\mu=135$ deg (Fig.3.a). The influence of the ship's speed for heave response is on $\omega=0.5-1.25$ rad/s at follow wave (Fig.3.b); it is negligible at beam wave (Fig.3.c) and is on $\omega=0.25-1$ rad/s at head wave (Fig.3.d).

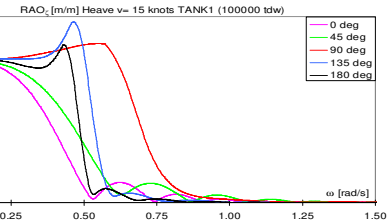


Fig.3.a. $RAO_3[\text{m/m}]$, TK1, $d_m=15\text{m}$, $v=15\text{kn}$

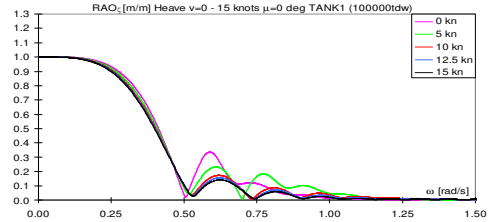


Fig.3.b. $RAO_3[\text{m/m}]$, TK1, $\mu=0$ deg, $v=0-15\text{kn}$

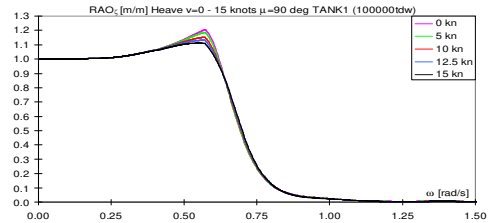


Fig.3.c. $RAO_3[\text{m/m}]$, TK1, $\mu=90$ deg, $v=0-15\text{kn}$

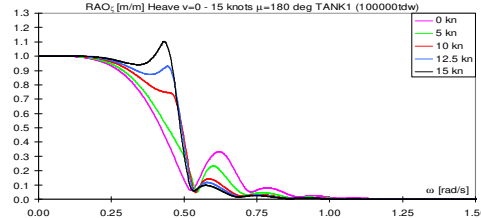


Fig.3.d. $RAO_3[\text{m/m}]$, $\text{TK1}, \mu=180 \text{ deg}, v=0-15\text{kn}$

Figs.4.a-d present a selection of pitch RAO_5 for the loading case TK1. The maximum pitch results at head wave, and is very reduced at beam wave (Figs.4.a,c). The influence of the ship's speed for pitch response is on $\omega=0.25-1.25 \text{ rad/s}$ at follow and head waves (Figs.4.b,d).

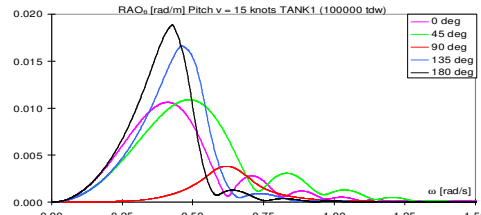


Fig.4.a. $RAO_5[\text{rad/m}]$, $\text{TK1}, d_m=15\text{m}, v=15\text{kn}$

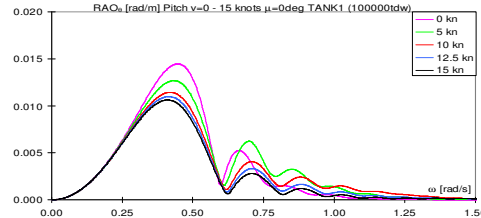


Fig.4.b. $RAO_5[\text{rad/m}]$, $\text{TK1}, \mu=0 \text{ deg}, v=0-15\text{kn}$

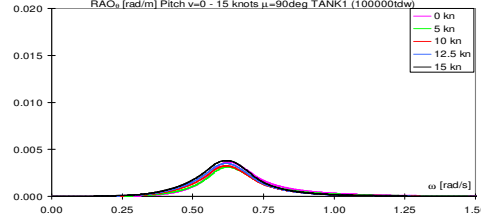


Fig.4.c. $RAO_5[\text{rad/m}]$, $\text{TK1}, \mu=90 \text{ deg}, v=0-15\text{kn}$

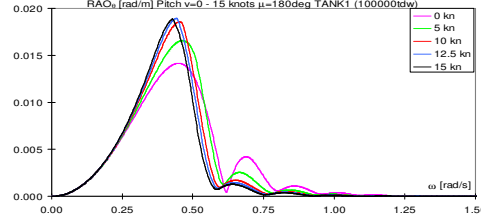


Fig.4.d. $RAO_5[\text{rad/m}]$, $\text{TK1}, \mu=180 \text{ deg}, v=0-15\text{kn}$

Figs.5.a-d present a selection of roll RAO_4 for the loading case TK1. The maximum roll results at beam wave (Figs.5.a,b,c); it is smaller at quartering wave and zero at follow and head wave. The influence of the ship's speed for roll response is on $\omega=0.25-0.75 \text{ rad/s}$ at aft and fore quarter waves (Figs.5.b,c); it is negligible at beam wave. Due to the significant changes of the natural roll period function to the vertical position of the gravity centre $z_G=8-14 \text{ m}$ (Table 2.a), $T_4=9.631-17.564 \text{ s}$ ($\omega_4=0.652-0.358 \text{ rad/s}$), the maximum roll RAO_4 ($\mu=90$) is for $z_G=8\text{m}$ (Figs.5.d), due to the fact that the roll hydrodynamic damping decreases when the frequency increases [6],[14].

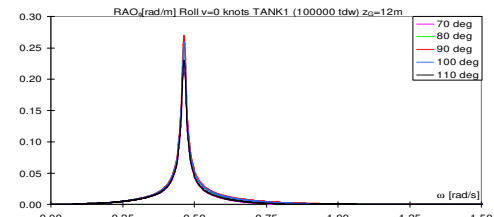


Fig.5.a. $RAO_4[\text{rad/m}]$, $\text{TK1}, z_G=12\text{m}, v=0\text{kn}$

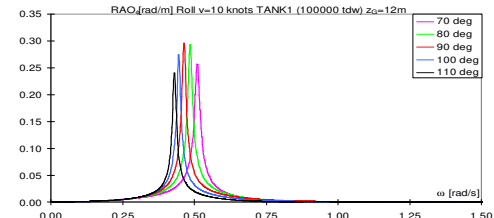


Fig.5.b. $RAO_4[\text{rad/m}]$, $\text{TK1}, z_G=12\text{m}, v=10\text{kn}$

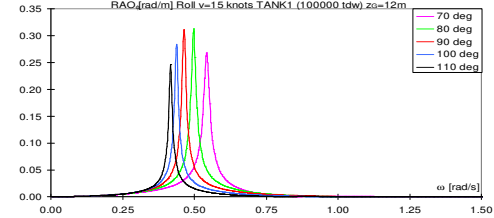


Fig.5.c. $RAO_4[\text{rad/m}]$, $\text{TK1}, z_G=12\text{m}, v=15\text{kn}$

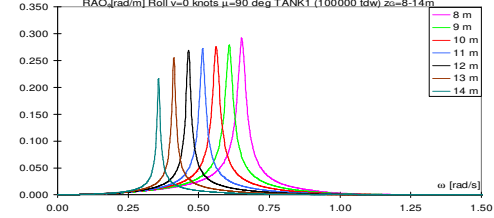


Fig.5.d. RAO_4 , $\text{TK1}, \mu=90, z_G=8-14\text{m}, v=0\text{kn}$

3.2 Loading case TK2

Figs.6.a-d present a selection of heave RAO_3 for the loading case TK2. The maximum heave results at beam wave (Fig.6.a). The influence of the ship's speed for heave response is on $\omega=0.55-1.3$ rad/s at follow wave (Fig.6.b); it is negligible at beam wave (Fig.6.c) and is on $\omega=0.1-1.25$ rad/s at head wave (Fig.6.d).

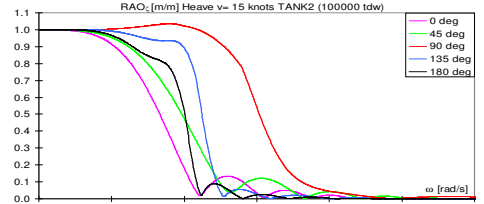


Fig.6.a. RAO_3 [m/m],TK2, d_m =10m, v =15kn

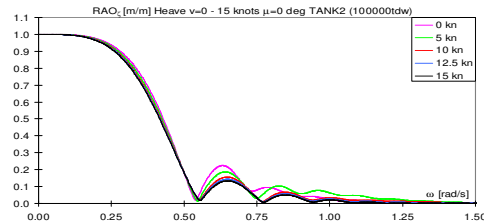


Fig.6.b. RAO_3 [m/m],TK2, μ =0 deg, v =0-15kn

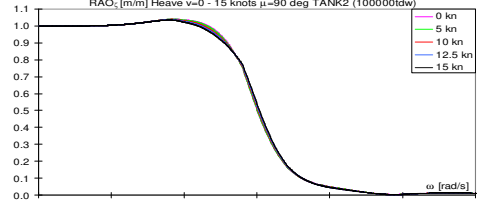


Fig.6.c. RAO_3 [m/m],TK2, μ =90 deg, v =0-15kn

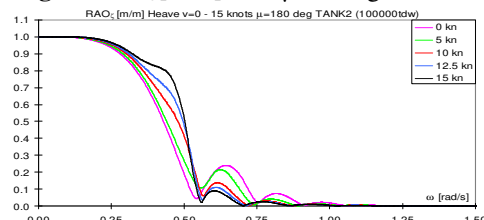


Fig.6.d. RAO_3 [m/m],TK2, μ =180 deg, v =0-15kn

Figs.7.a-d present a selection of pitch RAO_5 for the loading case TK2. The maximum pitch results at head wave and is very reduced at beam wave (Figs.7.a,c). The influence of the ship's speed for pitch response is on $\omega=0.2-1.3$ rad/s at follow and head wave (Figs. 7.b,d).

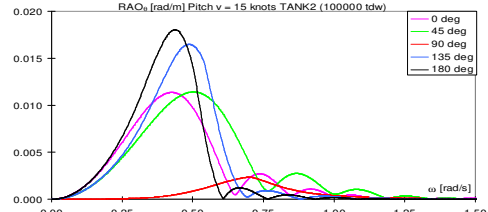


Fig.7.a. RAO_5 [rad/m],TK2, d_m =10m, v =15kn

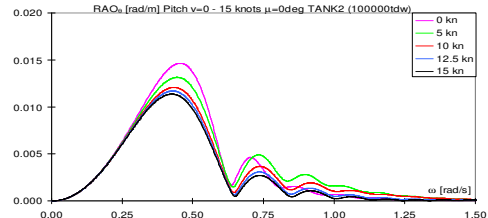


Fig.7.b. RAO_5 [rad/m],TK2, μ =0 deg, v =0-15kn

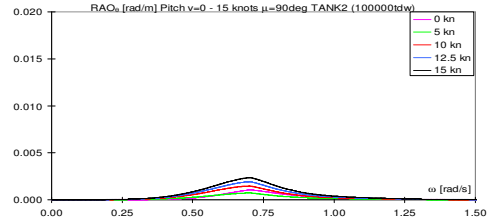


Fig.7.c. RAO_5 [rad/m],TK2, μ =90 deg, v =0-15kn

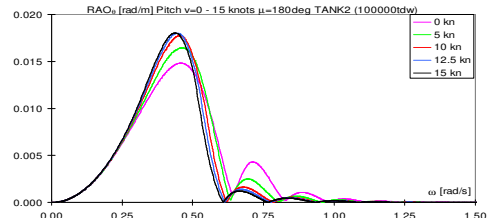
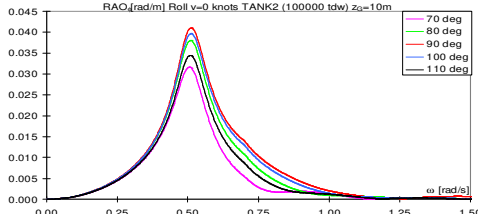
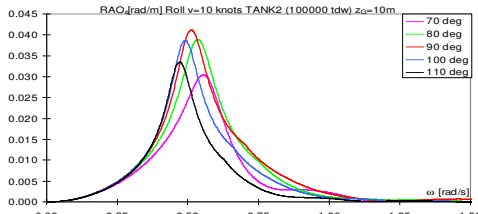
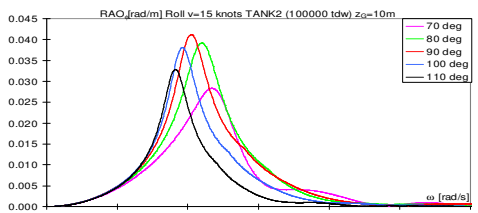
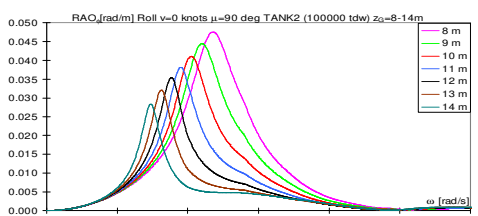


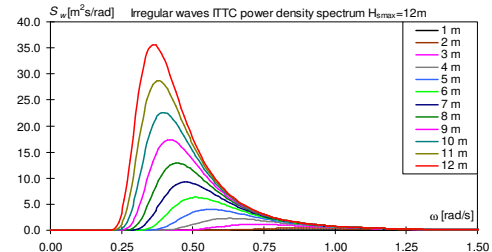
Fig.7.d. RAO_5 [rad/m],TK2, μ =180 deg, v =0-15kn

Figs.8.a-d present a selection of roll RAO_4 for the loading case TK2. The maximum roll results at beam wave (Figs.8.a,b,c); it is zero at follow and head wave. In comparison to case TK1 (Figs.5.a,b,c), in this case the roll response has a wider frequency band. The influence of the ship's speed for roll response is on $\omega=0.25-1.25$ rad/s at quarter waves (Figs.8.b,c) and is negligible at beam wave. Analogously to case TK1, the natural roll period changes for $z_G=8-14$ m (Table 2.b), $T_4=10.468-16.846$ s ($\omega_4=0.600-0.373$ rad/s), so that the maximum roll RAO_4 ($\mu=90$) is for $z_G=8$ m (Fig.8.d), being significantly smaller for $z_G=14$.

Fig.8.a. $RAO_4[\text{rad/m}]$, TK2, $z_G=10\text{m}$, $v=0\text{kn}$ Fig.8.b. $RAO_4[\text{rad/m}]$, TK2, $z_G=10\text{m}$, $v=10\text{kn}$ Fig.8.c. $RAO_4[\text{rad/m}]$, TK2, $z_G=10\text{m}$, $v=15\text{kn}$ Fig.8.d. $RAO_4[\text{rad/m}]$, TK2, $\mu=90$, $z_G=8-14\text{m}$, $v=0\text{kn}$

4. DYNAMIC RESPONSE IN IRREGULAR WAVES

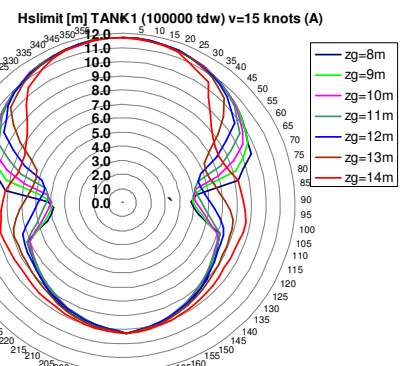
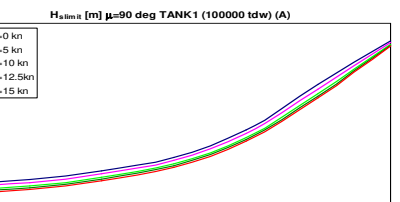
The dynamic response in irregular waves is computed using the RAO functions from section 3 and the ITTC wave power density spectrum from Fig.9 [10], for an unrestricted navigation condition $H_{smax}=12\text{m}$. Using equations (4)-(6), the RMS most probable amplitudes for heave, pitch, roll, motions and accelerations are obtained by DYN [6], module OSC. Based on the seakeeping criteria from equations (8)-(11), the polar diagrams for navigation safety (7) are obtained.

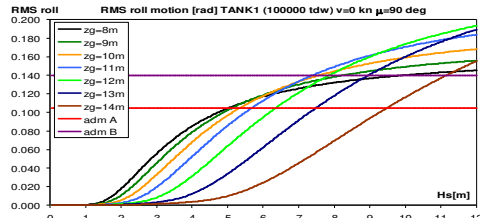
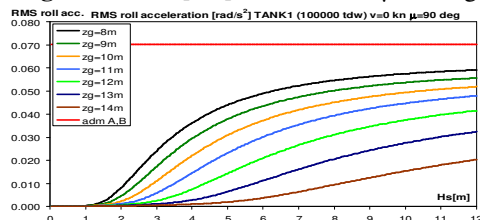
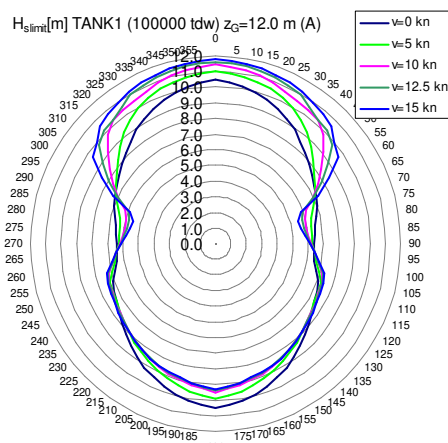
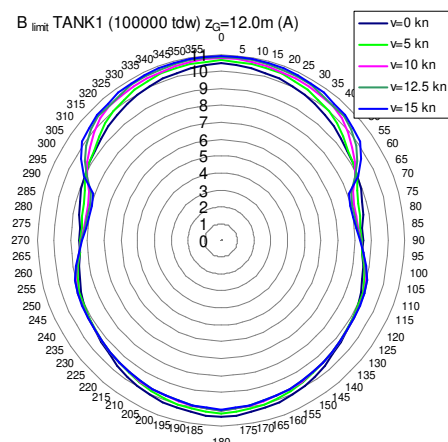
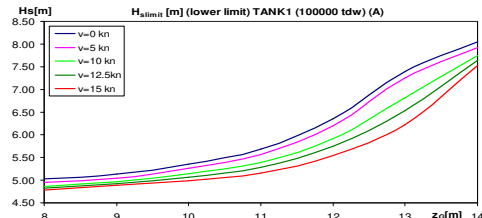
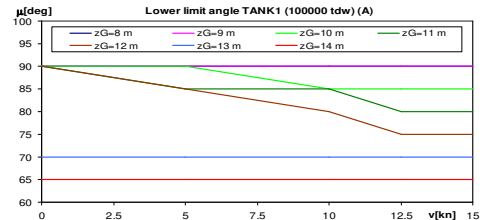
Fig.9. ITTC wave power density spectrum S_w [10]

4.1 Loading case TK1

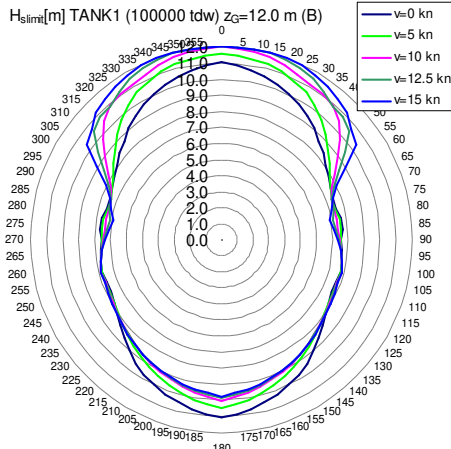
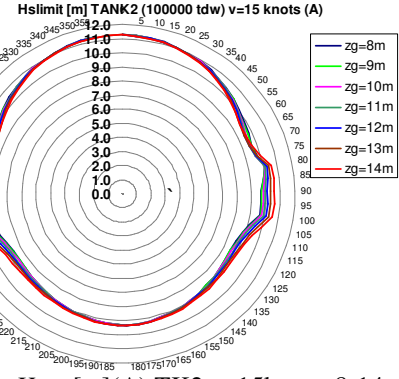
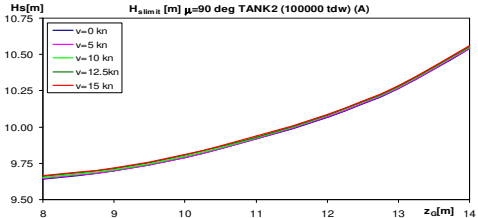
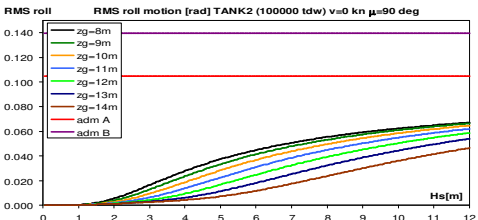
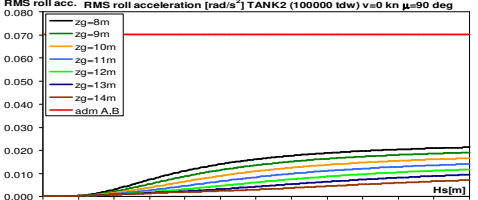
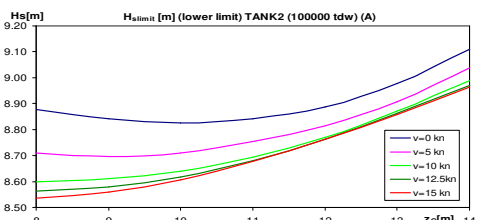
A selection of the statistic short-term results for the loading case TK1 (cargo) are included:

- Fig.10.a presents the H_{slimit} for $v=15\text{kn}$, $z_G=8-14\text{m}$, criteria A (Table 3) and Fig.10.b for $v=0-15\text{kn}$, $z_G=8-14\text{m}$, at beam sea;
- Figs.11.a,b present the most probable amplitudes for roll, $v=0\text{ kn}$, $z_G=8-14\text{m}$, at beam sea;
- Figs.12.a,b present the H_{slimit} and B_{limit} for $v=0-15\text{kn}$, $z_G=12\text{m}$, criteria A (Table 3);
- Figs.12.c,d present the lower H_{slimit} and heading angle, $v=0-15\text{kn}$, $z_G=8-14\text{m}$, criteria A;
- Fig.13 presents the H_{slimit} for $v=0-15\text{kn}$, $z_G=12\text{m}$, criteria B (Table 3);
- Tables 4.a,b present the H_{slimit} and B_{limit} for $v=0-15\text{kn}$, $z_G=8-14\text{m}$, criteria A and B.

Fig.10.a. $H_{slimit}[\text{m}]$ (A), TK1, $v=15\text{kn}$, $z_G=8-14\text{m}$ Fig.10.b. $H_{slimit}[\text{m}]$ (A), TK1, $v=0-15\text{kn}$, $\mu=90\text{deg}$

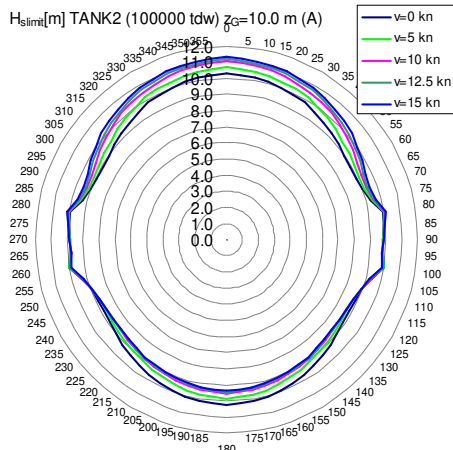
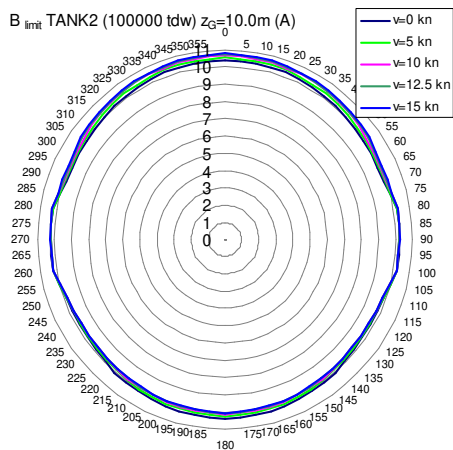
Fig.11.a. RMS_{roll}[rad], TK1, $v=0\text{kn}$, $\mu=90\text{deg}$ Fig.11.b. RMS_{acc}[rad/s²], TK1, $v=0\text{kn}$, $\mu=90\text{deg}$ Fig.12.a. $H_{slimit}[\text{m}]$ (A), TK1, $v=0-15\text{kn}$, $z_G=12\text{m}$ Fig.12.b. B_{limit} (A), TK1, $v=0-15\text{kn}$, $z_G=12\text{m}$ Fig.12.c. $H_{slimit}[\text{m}]$ (A) lower, TK1, $v=0-15\text{kn}$ Fig.12.d. Lower limit angle (A), TK1, $z_G=8-14\text{m}$ Table 4.a. $H_{slimit}[\text{m}]$, B_{limit} (A), TK1, $d_m=15\text{m}$

$v[\text{kn}]$	$z_G[\text{m}]$	$H_{slimit}[\text{m}]$	B_{limit}	Criterion
0	8	5.031-10.452	7.61-10.43	roll.mot.
	9	5.126-10.452	7.68-10.43	roll.mot.
	10	5.344-10.452	7.83-10.43	roll.mot.
	11	5.679-10.452	8.05-10.43	roll.mot.
	12	6.351-10.452	8.47-10.43	roll.mot.
	13	7.390-10.452	9.10-10.43	heave mot.
5	8	4.946-10.942	7.56-10.61	roll.mot.
	9	5.043-10.942	7.62-10.61	roll.mot.
	10	5.262-10.942	7.77-10.61	roll.mot.
	11	5.569-10.942	7.98-10.61	roll.mot.
	12	6.197-10.942	8.38-10.61	roll.mot.
	13	7.251-10.942	9.03-10.61	heave mot.
10	8	4.864-11.387	7.50-10.77	roll.mot.
	9	4.961-11.387	7.56-10.77	roll.mot.
	10	5.138-11.387	7.69-10.77	roll.mot.
	11	5.392-11.387	7.86-10.77	roll.mot.
	12	5.909-11.387	8.20-10.77	roll.mot.
	13	6.812-11.387	8.76-10.77	roll.mot.
12.5	8	4.823-11.574	7.47-10.84	roll.mot.
	9	4.920-11.574	7.54-10.84	roll.mot.
	10	5.061-11.574	7.63-10.84	roll.mot.
	11	5.285-11.574	7.79-10.84	roll.mot.
	12	5.745-11.574	8.10-10.84	roll.mot.
	13	6.528-11.574	8.59-10.84	roll.mot.
15	8	7.637-11.574	9.21-10.84	heave mot.
	9	4.783-11.725	7.44-10.90	roll.mot.
	10	4.880-11.725	7.51-10.90	roll.mot.
	11	4.985-11.725	7.58-10.90	roll.mot.
	12	5.156-11.725	7.70-10.90	roll.mot.
	13	6.219-11.725	8.39-10.90	roll.mot.
	14	7.521-11.725	9.16-10.90	heave mot.

Fig.13. H_{slimit} [m](B), TK1, $v=0-15\text{kn}$, $z_G=12\text{m}$ Fig.14.a. H_{slimit} [m](A), TK2, $v=15\text{kn}$, $z_G=8-14\text{m}$ Fig.14.b. H_{slimit} [m](A), TK2, $v=0-15\text{kn}$, $\mu=90\text{deg}$ Fig.15.a. RMS_4 [rad], TK2, $v=0\text{kn}$, $\mu=90\text{deg}$ Fig.15.b. RMS_{4c} [rad/s^2], TK2, $v=0\text{kn}$, $\mu=90\text{deg}$ Fig.16.c. H_{slimit} [m](A) lower, TK2, $v=0-15\text{kn}$

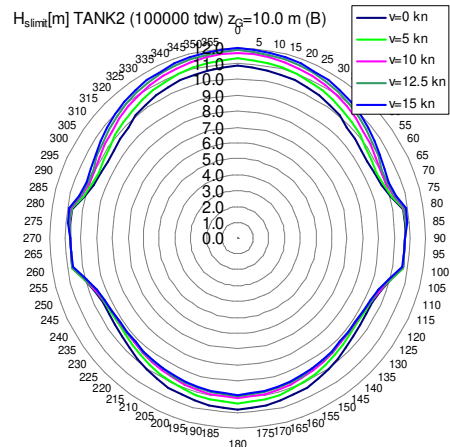
4.2 Loading case TK2

A selection of the statistic short-term results for the loading case TK2 (ballast) are included:
- Fig.14.a presents the H_{slimit} for $v=15\text{kn}$, $z_G=8-14\text{m}$, criteria A (Table 3) and Fig.14.b for $v=0-15\text{kn}$, $z_G=8-14\text{m}$, at beam sea;
- Figs.15.a,b present the most probable amplitudes for roll motion and acceleration, $v=0\text{kn}$, $z_G=8-14\text{m}$, at beam sea;
- Figs.16.a,b present the H_{slimit} and B_{limit} for $v=0-15\text{kn}$, $z_G=10\text{m}$, criteria A (Table 3);
- Fig.16.c presents the lower H_{slimit} for $v=0-15\text{kn}$, $z_G=8-14\text{m}$, criteria A (Table 3);
- Fig.17 presents the H_{slimit} for $v=0-15\text{kn}$, $z_G=10\text{m}$, criteria B (Table 3);
- Tables 5.a,b present the H_{slimit} and B_{limit} for $v=0-15\text{kn}$, $z_G=8-14\text{m}$, criteria A and B.

Fig.16.a. $H_{slimit}[m](A)$, TK2, $v=0-15\text{kn}$, $z_G=10\text{m}$ Fig.16.b. $B_{limit}(A)$, TK2, $v=0-15\text{kn}$, $z_G=10\text{m}$ Table.5.a. $H_{slimit}[m]$, B_{limit} (A), TK2, $d_m=10\text{m}$

$v[\text{kn}]$	$z_G[\text{m}]$	$H_{slimit}[\text{m}]$	B_{limit}	Criterion
0	8	8.879-10.259	9.81-10.36	heave mot.
	9	8.843-10.259	9.79-10.36	heave mot.
	10	8.826-10.259	9.78-10.36	heave mot.
	11	8.842-10.259	9.79-10.36	heave mot.
	12	8.888-10.259	9.81-10.36	heave mot.
	13	8.977-10.361	9.85-10.40	heave mot.
5	14	9.111-10.601	9.92-10.48	heave mot.
	8	8.709-10.654	9.73-10.50	heave mot.
	9	8.695-10.654	9.72-10.50	heave mot.
	10	8.709-10.654	9.73-10.50	heave mot.
	11	8.755-10.654	9.75-10.50	heave mot.
	12	8.816-10.654	9.78-10.50	heave mot.
	13	8.907-10.654	9.82-10.50	heave mot.
15	14	9.038-10.654	9.88-10.50	heave mot.

10	8	8.599-11.014	9.67-10.64	heave mot.
	9	8.609-11.014	9.68-10.64	heave mot.
	10	8.640-11.014	9.69-10.64	heave mot.
	11	8.694-11.014	9.72-10.64	heave mot.
	12	8.770-11.014	9.75-10.64	heave mot.
	13	8.871-11.014	9.80-10.64	heave mot.
12.5	14	8.988-11.014	9.86-10.64	heave mot.
	8	8.564-11.164	9.66-10.69	heave mot.
	9	8.579-11.164	9.66-10.69	heave mot.
	10	8.617-11.164	9.68-10.69	heave mot.
	11	8.681-11.164	9.71-10.69	heave mot.
	12	8.763-11.164	9.75-10.69	heave mot.
15	13	8.862-11.164	9.80-10.69	heave mot.
	14	8.971-11.164	9.85-10.69	heave mot.
	8	8.537-11.280	9.64-10.73	heave mot.
	9	8.560-11.280	9.65-10.73	heave mot.
	10	8.607-11.280	9.68-10.73	heave mot.
	11	8.677-11.280	9.71-10.73	heave mot.
17	12	8.763-11.280	9.75-10.73	heave mot.
	13	8.858-11.280	9.80-10.73	heave mot.
	14	8.964-11.280	9.85-10.73	heave mot.

Fig.17. $H_{slimit}[m](B)$, TK2, $v=0-15\text{kn}$, $z_G=10\text{m}$ Table.5.b. $H_{slimit}[m]$, B_{limit} (B), TK2, $d_m=10\text{m}$

$v[\text{kn}]$	$z_G[\text{m}]$	$H_{slimit}[\text{m}]$	B_{limit}	Criterion
0	8	9.512-10.848	10.08-10.58	heave mot.
	9	9.463-10.848	10.07-10.58	heave mot.
	10	9.439-10.848	10.06-10.58	heave mot.
	11	9.447-10.848	10.06-10.58	heave mot.
	12	9.486-10.961	10.07-10.62	heave mot.
	13	9.567-11.137	10.10-10.68	heave mot.
15	14	9.690-11.397	10.15-10.78	heave mot.
	8	9.083-11.917	9.90-10.97	heave mot.
	9	9.101-11.917	9.91-10.97	heave mot.
	10	9.146-11.917	9.93-10.97	heave mot.
	11	9.215-11.917	9.97-10.97	heave mot.
	12	9.291-11.917	10.00-10.97	heave mot.
	13	9.385-11.917	10.04-10.97	heave mot.
17	14	9.496-11.917	10.08-10.97	heave mot.

5. CONCLUSIONS

For a 100000 tdw tanker [8] (Fig.1,Tables 1, 2), based on our own code DYN [6], with theoretical model (1)-(6), a parametric study has been developed (Δ, z_G, v, μ, H_s) for the dynamic response in regular and irregular waves, resulting the operation capabilities limits (7), by seakeeping criteria (8)-(11) (Table 3).

From the regular wave's dynamic response (for 2590 cases), the response amplitude operators are obtained (Figs.3-8). The heave RAO_3 is maximal at quarter-head wave for TK1 and at beam wave for TK2. The pitch RAO_5 is maximal at head waves for both loading cases, and is much reduced at beam waves. The roll RAO_4 is maximal at beam waves, with zero values at follow and head waves.

For reference $v=0$ kn, $\mu=90$ deg. (Figs. 5.d, 8.d.), the maximum roll RAO_4 is for $z_G=8$ m and decreases for $z_G=9-14$ m, due to the increase of the hydrodynamic damping, while the natural period increase (Tables 2.a,b). The ship's speed influence is reduced at beam waves, being significant on the other heading angles.

From the irregular wave's dynamic response, in 621600 cases, the short-term most probable amplitudes RMS and the operation limits in terms of polar diagrams H_{slimit}, B_{limit} are obtained (Figs.10-17, Tables 4,5). The main restriction criteria are heave (9) and roll (10) motions for TK1 and only heave motion for TK2. The influence of the $z_G=8-14$ m over the roll RMS_4 , RMS_{ac4} is very significant (Figs.11,15), also affecting the vertical RMS_Z (8). The z_G influence on operation limits is mainly on beam and quarter sea (Figs.10,14).

The operation limits for criteria A are in the range: $H_{slimit}=4.783-11.725$ m ($B_{limit}=7.44-10.90$) for TK1, $H_{slimit}=8.537-11.280$ m ($B_{limit}=9.64-10.73$) for TK2. If the reduced criteria B (Table 3) are considered, the operation limits are improving: $H_{slimit}=7.469-12$ m ($B_{limit}=9.13-11$) for TK1, $H_{slimit}=9.083-11.917$ m ($B_{limit}=9.90-10.97$) for TK2. A significant influence of the ship's speed and gravity centre position is recorded (Figs.12,13,16,17, Tables 4,5).

Further studies will extend this analysis on other ship types and loading conditions.

Acknowledgements

This study and the program DYN [6] are developed at the Naval Architecture Research Centre, from "Dunarea de Jos" University of Galati.

REFERENCES

- [1]. **Bertram, V.**, "Practical ship hydrodynamics", Butterworth Heinemann, Oxford, 2000.
- [2]. **Bidoae, I., Ionas, O.**, "Naval architecture complements", Porto-Franco, Galati, 1998.
- [3]. **Burlacu, E., Domnisoru, L., Obreja, D.**, "Seakeeping prediction of a survey vessel operating in the Caspian Sea", The 37th International Conference on Offshore Mechanics and Arctic Engineering, ASME, Paper No. OMAE 2018-77126, Madrid, 2018.
- [4]. **BV**, "Rules", Bureau Veritas, Paris, 2019.
- [5]. **DNV-GL**, "Rules", Det Norske Veritas – Germanischer Lloyd, 2019.
- [6]. **Domnisoru, L.**, "Ship dynamics. Oscillations and vibrations", Technical Publishing House, Bucharest 2001.
- [7]. **Domnisoru, L., Rubanenco, I., Obreja, D.**, "The experimental and numerical linear and non-linear analyses of oscillations response, based on a scaled ITTC type ship model", The Annals of "Dunarea de Jos" University of Galati, Fascicle XI Shipbuilding, pp.75-84, 2013.
- [8]. **Dumitru, D.**, "Compendium of ships forms", "Dunarea de Jos" University Foundation Publishing House, Galati, 2014.
- [9]. **Gasparotti, C., Domnisoru, L., Obreja, D.**, "The oscillations analysis in head waves of a tractor-tug model by experimental and numerical methods", 16th SGEM GeoConference on Water Resources,(3), pp.877-884, Albena, 2016.
- [10]. **ITTC**, "Recommended procedures and guidelines. Seakeeping", The International Towing Tank Conference, 2011.
- [11]. **Obreja, D.**, "Ship theory. Concepts and methods for the navigation performances analysis", E.D.P. Publishing House, Bucharest, 2005.
- [12]. **Obreja, D., Nabergoj, R., Crudu, L., Domnisoru, L.**, "Seakeeping performance of a Mediterranean fishing vessel", IMAM, Maritime Transportation and Harvesting of Sea Resources, pp.483-491, Lisbon, 2017.
- [13]. **Solas**, "International convention for the safety of life at sea", IMO, 2014.
- [14]. **Voitkunski, Y.I.**, "Ship theory handbook", Sudostroenie, Sankt Petersburg, 1985.

Paper received on August 20th, 2019